NRIAG Journal of Astronomy and Geophysics (2017) 6, 148–161

National Research Institute of Astronomy and Geophysics

NRIAG Journal of Astronomy and Geophysics

www.elsevier.com/locate/nrjag

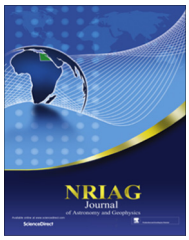

REVIEW ARTICLE

Utilization of airborne gamma ray spectrometric data for radioactive mineral exploration of G.Abu Had – G.Umm Qaraf area, South Eastern Desert, Egypt

A.A. Elkhadragy [a], A.A. Ismail [b], M.M. Eltarras [b], A.A. Azzazy [b,*]

[a] *Geology Department, Faculty of Science, Zagazig University, Sharkia, Egypt*
[b] *Exploration Division, Nuclear Material Authority, Cairo, Egypt*

Received 9 August 2016; revised 27 November 2016; accepted 2 December 2016
Available online 26 December 2016

KEYWORDS

Airborne gamma ray spectrometry;
Statistical analysis;
Radioactive anomalies;
Mineral exploration

Abstract Airborne gamma-ray spectrometry method is a powerful tool for geological mapping, mineral exploration and environmental monitoring. Qualitative and quantitative interpretations were performed on the airborne spectrometric data of G.Abu Had – G.Umm Qaraf area, South Eastern Desert, Egypt. Special attention is focused in this paper to discuss the distribution of k, eTh, eU and TC maps. Also there are statistical analyses for the radioactive content for the rock units of the studied area. Anomalies of high radioactive content were calculated and studied by field ground follow-up. The younger granites, Natach volcanic, gneissose granites and pegmatite rocks are the highly content of uranium in the studied area.

Contents

* Corresponding author.
E-mail address: semsema198512@gmail.com (A.A. Azzazy).

Peer review under responsibility of National Research Institute of Astronomy and Geophysics.

http://dx.doi.org/10.1016/j.nrjag.2016.12.001

1. Introduction

The gamma-ray spectrometric measurements give qualitative and quantitative determination of the individual radiation elements in the rocks and soils, and assist considerably in the search for uranium ores and therefore are of great importance to mineral exploration in general and geological mapping in particular. The disintegration of natural radioactive elements is accompanied by the emission of the three radioactive decay types: alpha particles, beta particles and electromagnetic radiation. Gamma rays, in contrast to alpha and beta particles, have no mass or charge and therefore, form the most penetrating radiation. The rays are not affected by electric or magnetic fields, but travel at the speed of light and eject photoelectrons from certain materials (Essa, 2015). In airborne gamma-ray spectra, the photopeaks are the primary information about the geological and geophysical state of soil and subsurface rocks (Eugene, 2016). The present study deals essentially with the analysis and interpretation of aerial spectral gamma-ray survey data. The data interpretation would be supplemented by the consideration of all available previous geological and all information works in this area. In brief the proposed study has the following main objectives:

1. Analyzing gamma-ray spectrometric data for lithologic and geological refinement.
2. Studying radioactive data to delineate the economic locations and checked it with ground field follow-up.
3. Statistical analysis of the total count content for all rock units of the studied area.

Area is located in the southern part of the Eastern Desert of Egypt. It is about 100 km southwest Marsa Alam City. The surveyed area is bounded by latitudes 24°–25°N and longitudes 34°–35°E with 1221 km^2 area (Fig. 1). More than 95% of the area is covered by crystalline basement (igneous and metamorphic rocks). Sedimentary rocks and wadi sediments cover small region. Quaternary sand and gravel extensively cover plains and wadis. The compiled geological map shows the available information about the surface geology. Faults, joints and foliation, in addition to lithologic boundaries, are the main features controlling the dendritic drainage pattern of the area.

2. Geological outline

The study area is a part of the Precambrian belt in the South Eastern Desert of Egypt. Proterozoic (igneous and metamorphic) and Phanerozoic rocks are exposed in the studied area as illustrated in the geological map (Fig. 2) that was modified after EGSMA (1997, 2001).

2.1. Quaternary sediments (Qw)

Detritus, sands, gravels, pebbles, cobbles and boulders are distributed all over the area and constitute the surficial cover in the main Wadis. They are generally formed by the weathering of the different types of rocks. Quaternary deposits are represented by wadi deposits (alluvial sediments) along the courses of wadis such as Wadi Natach at the center of the studied area and Wadi Hafafit at NE part of the area. Also there are wadies at south, north and central parts.

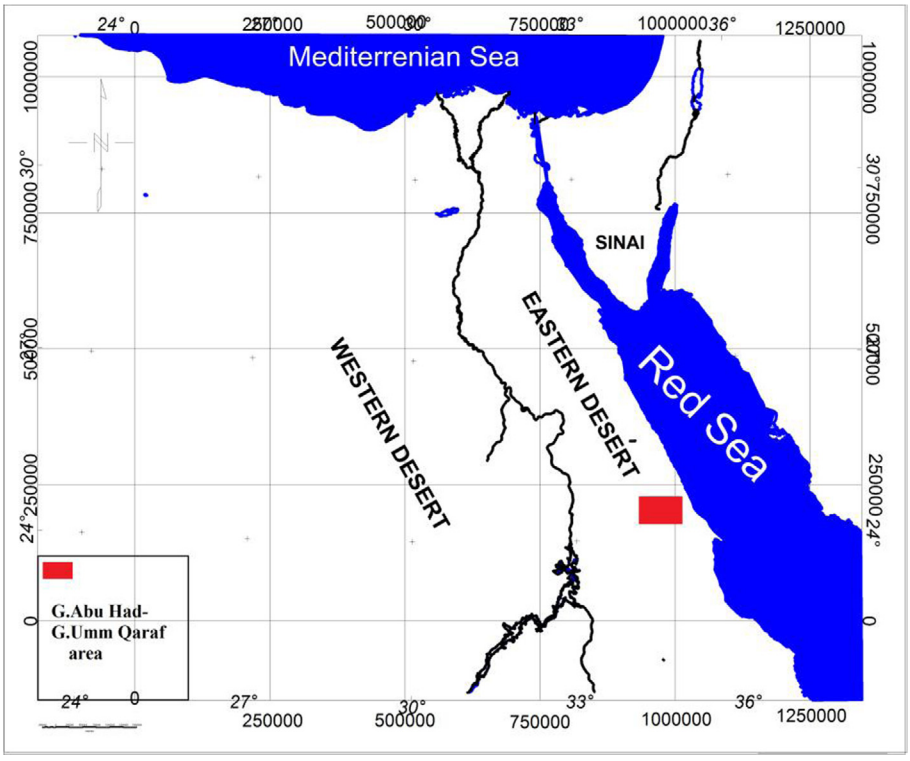

Figure 1 Location map of G.Abu Had-G.Umm Qaraf area, South Eastern Desert, Egypt.

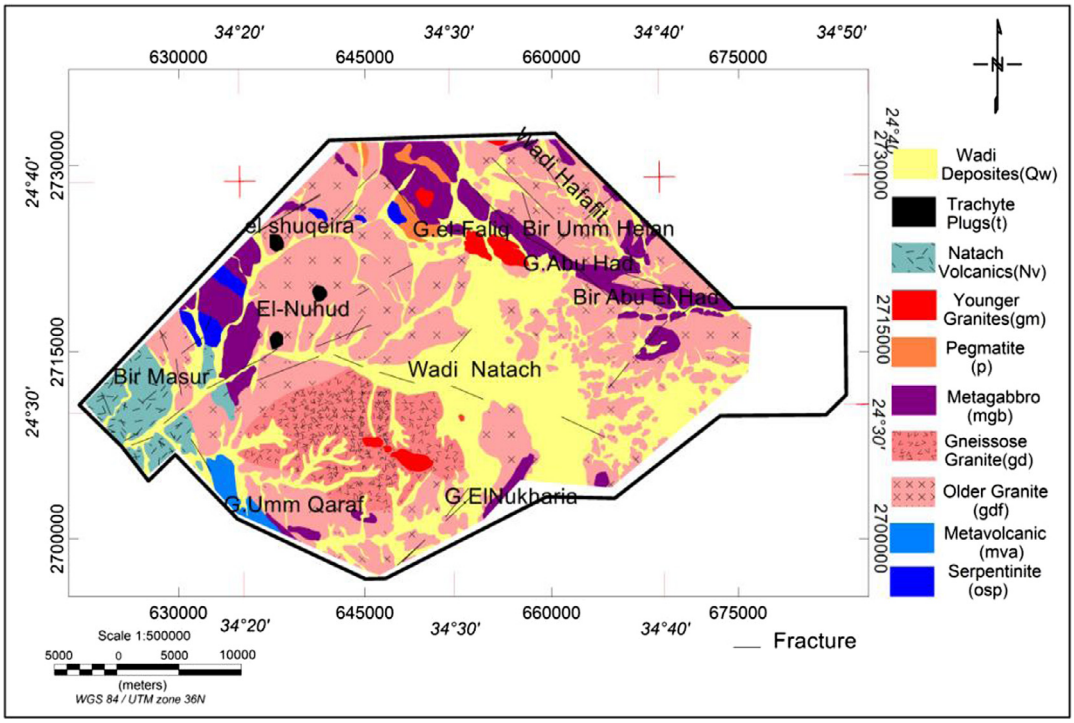

Figure 2 Geological map of G.Abu Had-G.Umm Qaraf area, South Eastern Desert, Egypt, after EGSMA (1997, 2001).

2.2. Trachyte plugs (T)

They are represented by trachyte plugs and sheets. They have exposure like spots at the west of the area. These trachyte plugs are located at El-Nuhud; they are fine-grained, massive and vary in color from dark gray to grayish brown.

2.3. Natach volcanics (Nv)

These volcanics are well exposed west of the area. They are basic to acidic alkaline, undeformed volcanic rocks. Wadi Natach volcanics acquired their name from the type locality, Wadi Natash, located at the western border of the basement complex at the South Eastern Desert of Egypt. They were extensively erupted during the upper Cretaceous associated with the regional uplift preceding the northern Red Sea rifting. Surface manifestation of these volcanics is cropped out in separate locations in the study area as alkaline basalts and numerous of small trachytic intrusions (Hashad et al., 1982).

2.4. Younger granites (gm)

The younger granitic rocks (alkali feldspar granites) are outcropping in northern and southern parts of the studied area with small exposure. The majorities of these intrusions are rounded or elongate parallel to the direction of the Red Sea and possess relatively sharp contacts with the surrounding rocks. The younger granites are exposed in the eastern side of G. El Faliq, Naslet Abu Gabir as well as northeast W. Abu Gherban. They are characterized by low to moderate topography (375 m), cover about 95 km^2, constituting some 45 in vol.% of the total exposed basement rocks and form elongated mass in NW-SE direction(Mostafa, 2013).

2.5. Pegmatite (P)

Pegmatite occurs as steeply dipping bodies of variables size. These rocks are very coarse grained mainly observed in the older granites near the contact with ophiolitic mélange. They are mainly composed of milky quartz, plagioclase with small pockets of mica. Also all the granitoid rocks of G. El Faliq are cut and crossed by several pegmatite bodies. These bodies are trending (NNE-SSW) and ranging in length from 50 m to several meters. Also, they occur as pockets or lenses (10–20 m in length) at the margin and the core of the gneisses rocks as well as ophiolitic mélange (Mostafa, 2013).

2.6. Metagabbro (mgb)

It is undifferentiated Intrusive metagabbro. It is exposed as limited outcrops at the western and northeastern parts of the studied area. It is composed of heterogeneous assemblage of rock types. They are mainly metamorphosed basic rocks including gabbro, norites, delorites, and basalts, in which the igneous textures are partly preserved.

2.7. Gneissose granites (gd)

Gneissose granites are highly mylonitized and dissected by several faults mostly oriented to NW-SE directions. They show a well developed planer banding, gneissosly and folding. Small size quartz and pegmatitic veins are common and seem to be

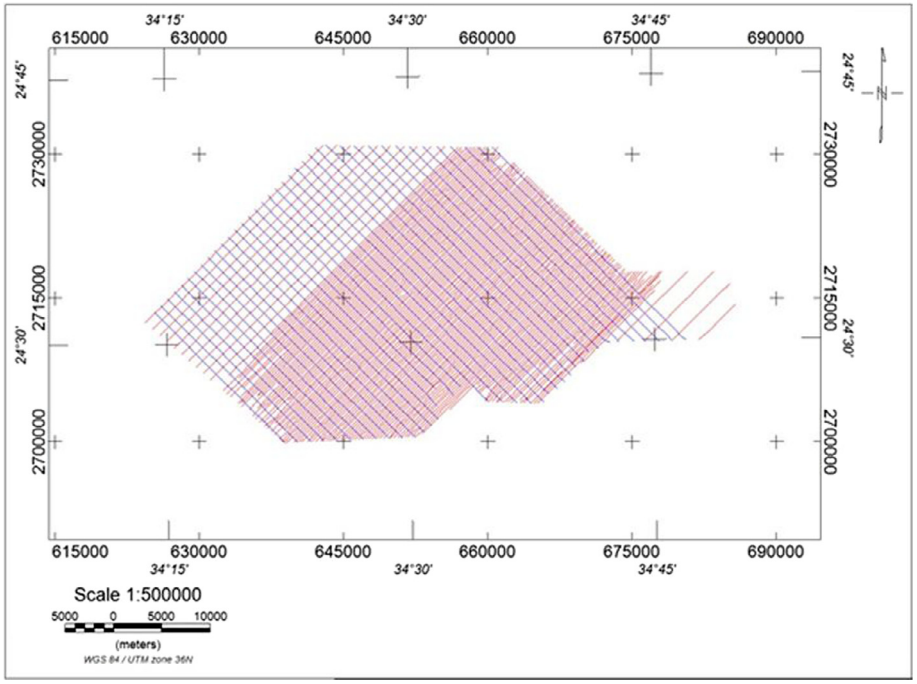

Figure 3 Airborne Survey Lines of G.Abu Had-G.Umm Qaraf area, South Eastern Desert, Egypt (after NMA, 2012).

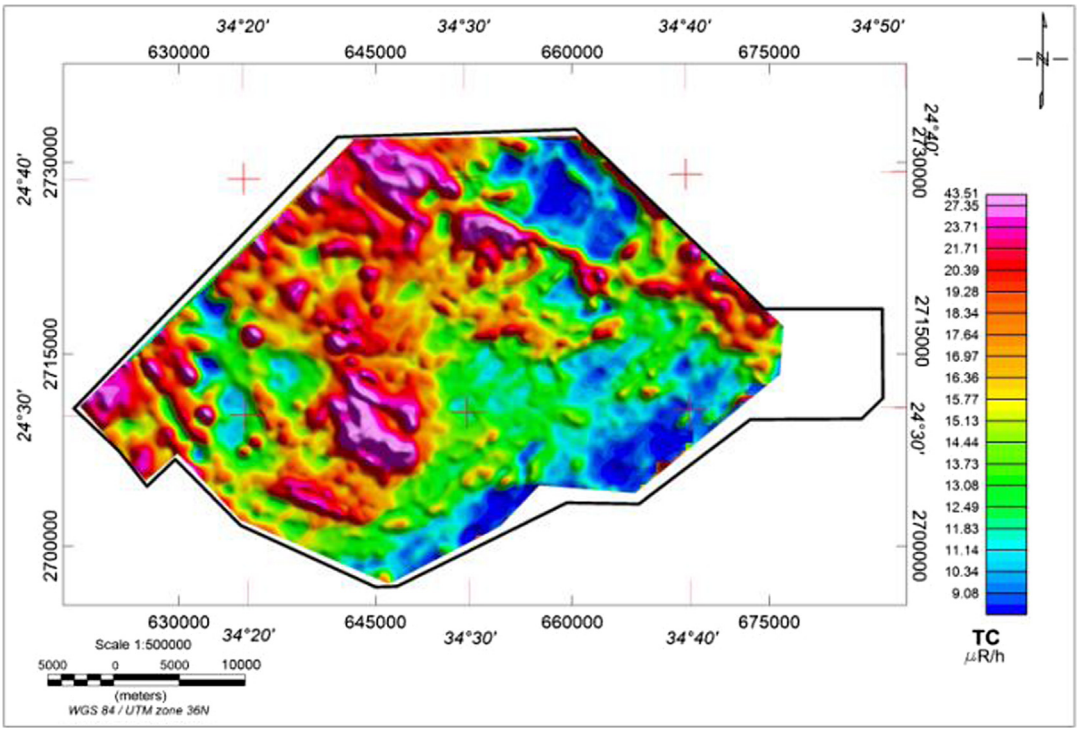

Figure 4 Total counts (μR/h) distribution image map of G.Abu Had-G.Umm Qaraf area, South Eastern Desert, Egypt.

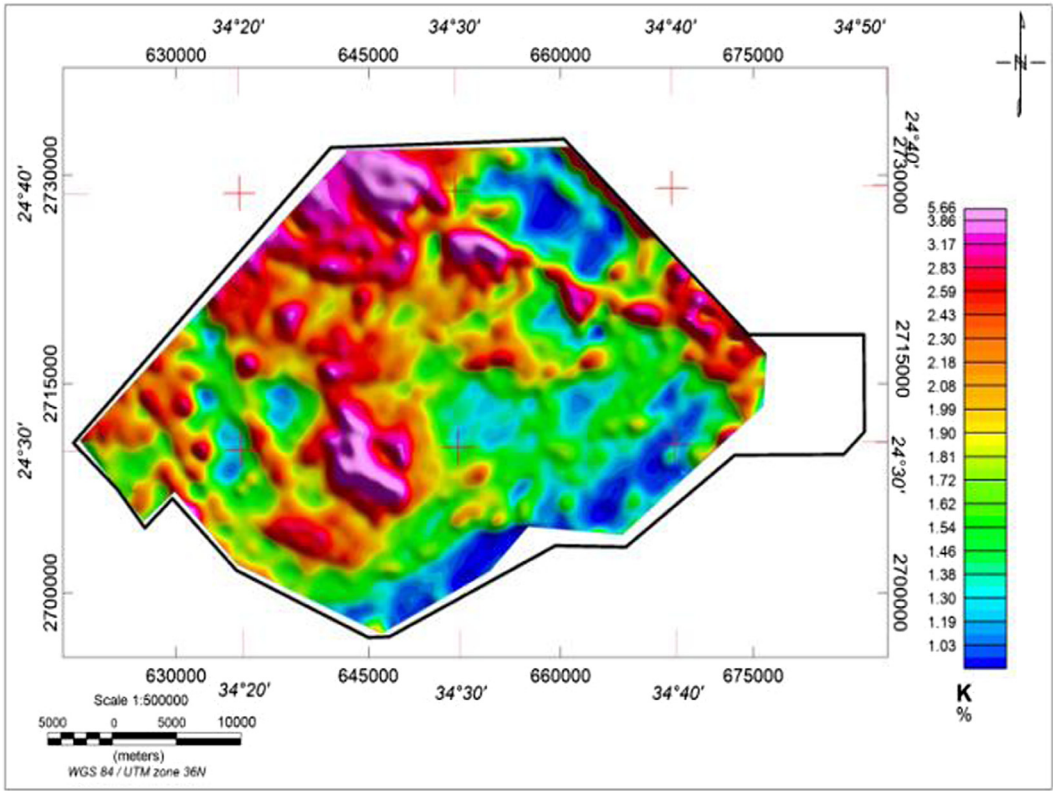

Figure 5 Potassium concentration (K %) distribution image map of G.Abu Had-G.Umm Qaraf area, South Eastern Desert, Egypt.

developed from the gneiss through mobilization and crystallization.

2.8. Older granites (gdf)

They are exposed as wide outcrops located around Wadi Hafafit at the northwestern and eastern parts and represented a wide exposure of G.Umm Qaraf at the southern part of the area.

It occupies the extreme eastern side of the G. El Faliq. Also they have a wide exposure around G.Umm Qaraf. It occurs along the contact between the ophiolitic mélange and the younger granites. The older granites are characterized by relatively low to-medium topography. In hand specimens they are whitish in color and characterized by medium to coarse grained and obvious biotite flakes (Mostafa, 2013).

2.9. Acidic metavolcanics (mva)

It is Intermediate to acidic metavolcanics and metepyroclastics. It is exposed in a small part in the area at the southwestern part. The metavolcanics constitute a pile of regionally-metamorphosed submarine lava flows of alternating basic, intermediate and acidic compositions.

2.10. Serpentinite (osp)

The ophiolitic rock in the area under study is represented by Serpentines (osp), talc carbonates and related rocks. Serpentinite, essentially formed after harzburgite and to a lesser extend after dunite and lherzolite, is frequently transformed into talc-carbonates particularly along thrust fault and shear zone. Outcrops are located as few masses at the west. Serpentinite at G. Faliq area occurs either as huge masses or small masses at the western part of the studied area (Fig. 2).

3. Airborne survey specification

The Egyptian Nuclear Materials Authority (NMA) in the year conducted a comprehensive airborne high resolution geophysical survey, over G.Abu Had-G.Umm Qaraf, South Eastern Desert, Egypt, along flight-lines oriented in NE-SW direction using 250 m line spacing for central and eastern part of the study area and 1000 m for the northern and western parts of the study area the tie-lines oriented in NW-SE direction using 1000 m line spacing for the whole area (Fig. 3). Nominal flying elevation was 100 m above ground surface (NMA, 2012).

4. Description of radioelement distribution map and their ratios

The radioelement images provide views of the overall patterns of elements and usually contain patterns related to various lithologies. The collected data involve the total count (TC), equivalent uranium (eU), equivalent thorium (eTh) and potassium concentration (K %) used to construct four image maps.

The lowest level (level 1 from bright blue to green) is encountered in the four radiometric maps with the southeastern and northeastern parts of the studied area. It is more or less having the same feature of less radiometric effect. The intermediate level (level 2 from green to yellow) is spread from central to southern parts of the studied area. This level is clear in the four radioactive maps. The highest level (level 3 from

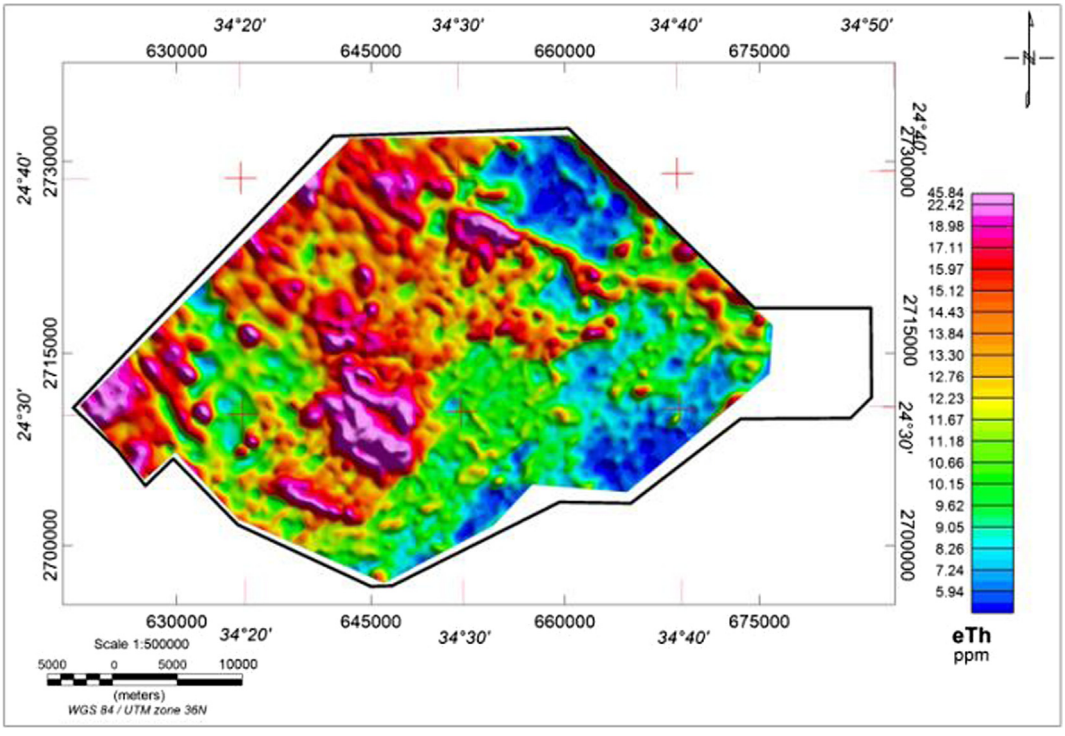

Figure 6 Equivalent Thorium (ppm) concentration image map of G.Abu Had-G.Umm Qaraf area, South Eastern Desert, Egypt.

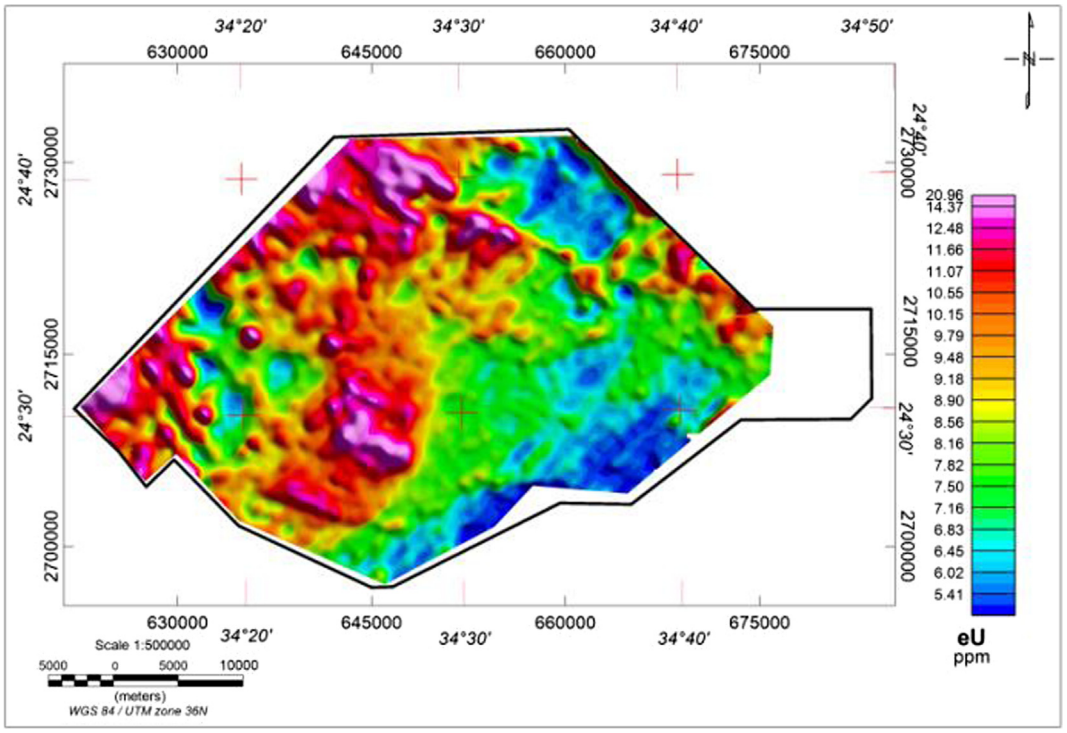

Figure 7 Equivalent Uranium concentration (ppm) image map of G.Abu Had-G.Umm Qaraf area, South Eastern Desert, Egypt.

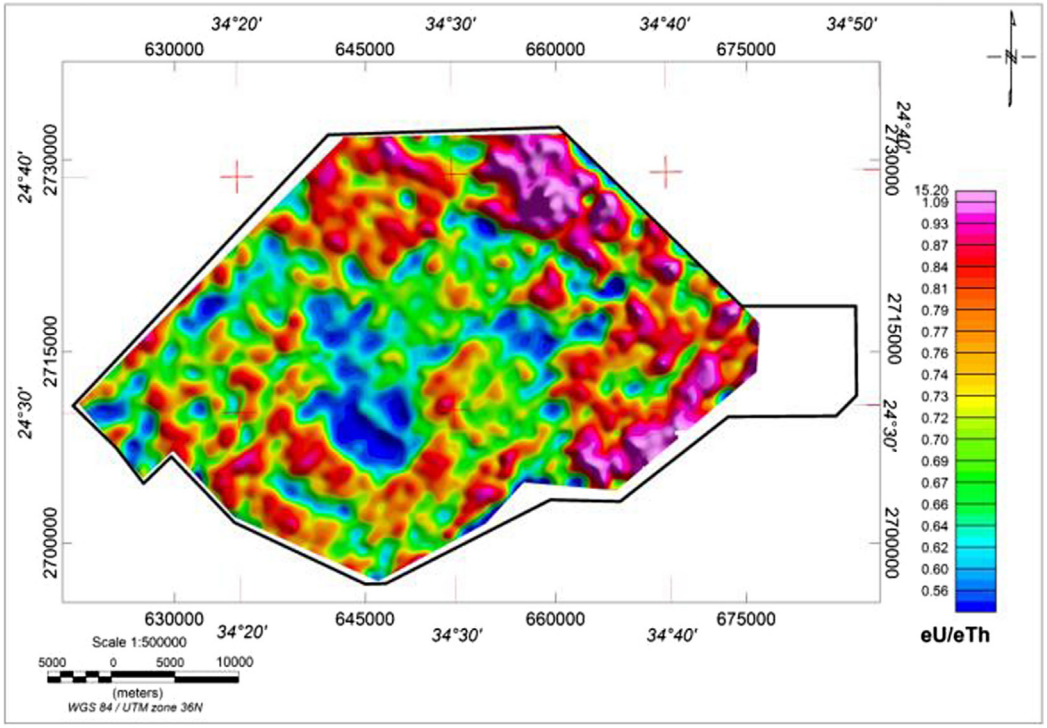

Figure 8 Equivalent Uranium/equivalent Thorium ratio (eU/eTh) image map of G.Abu Had-G.Umm Qaraf area, South Eastern Desert, Egypt.

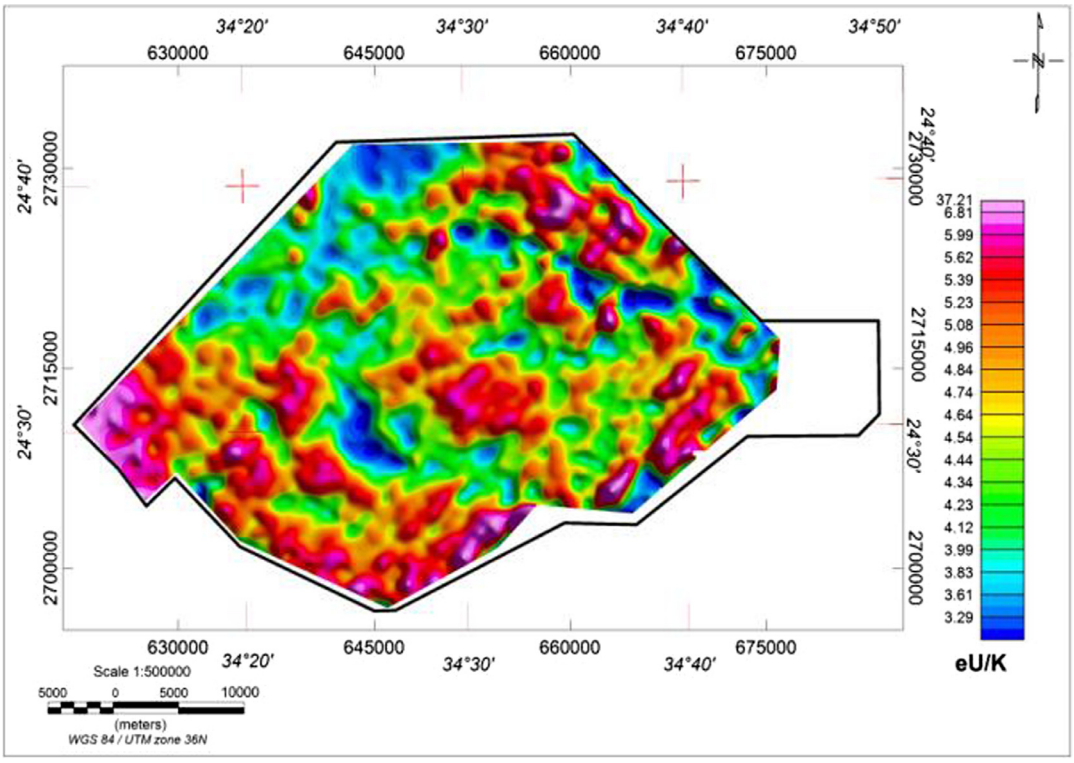

Figure 9 Equivalent Uranium/Potassium ratio (eU/K) image map of G.Abu Had-G.Umm Qaraf area, South Eastern Desert, Egypt.

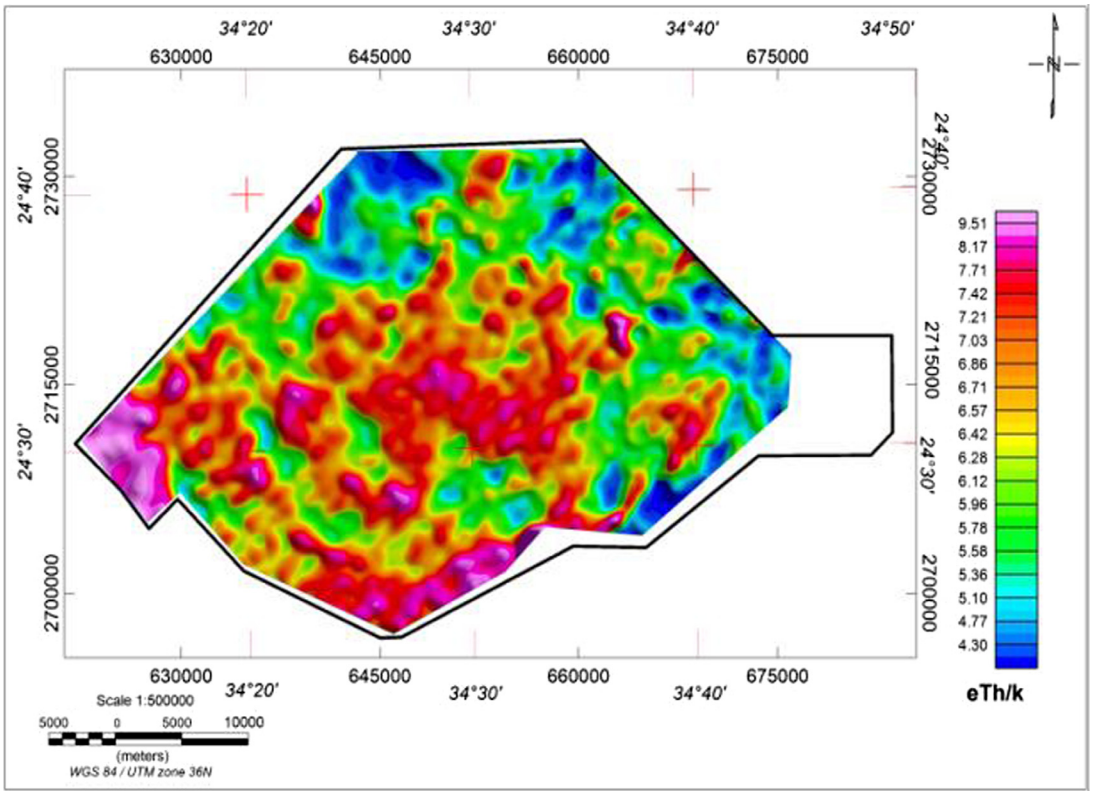

Figure 10 Equivalent Thorium/Potassium ratio (eTh/K) image map of G.Abu Had-G.Umm Qaraf area, South Eastern Desert, Egypt.

bright magenta to strong magenta) is associated mostly with a wide part of the basement rocks. This level in all spectrometric maps is related to the presence of younger granites, pegmatite, Natach volcanics and gneissos granite. It is found that the main effected trends in the radiometric maps are the Northwest-Southeast trend (Red Sea trend) and North Northwest (Atalla trend).

4.1. Total Count (TC) map

In the total count radiometric map (Fig. 4) there are general three major levels of radiation. The lowest level ranges from 8 to 11 μR/h and this range is represented by pale blue color. This range is correlated mainly with the Quaternary wadi sediments, serpentinities, metagabbro and older granites. The intermediate level (level 2) has color from yellow to bright green and it ranges from 12 to 16 μR/h. This range is correlated with parts of older granites, trachyte plugs and gneissos granites. The high level (level 3) ranges from 16.5 to 45 μR/h represented by the orange, red and magenta colors correlated mainly with Natach volcanic, younger granites and pegmatite.

4.2. Potassium (K %) Map

Potassium map (Fig. 5) shows three levels of K-concentrations. The first level here is represented by blue to bright green and ranges from 1.03% to 1.46%. This low level covers northeastern and southeastern parts of the studied area associated with Quaternary wadi sediments, metavolcanics, older granites and metagabbro rocks. The second level as intermediate level is drawn by green to orange colors. This level ranges from 1.46% to 2.30% and it is represented by parts of older granites and Natach volcanic and trachyte plugs.

The third level (highest one) ranges from 2.30% to 5.66% and has orange to magenta colors. This level is associated with younger granite at G. El Faliq, gneissose granites and pegmatite.

4.3. Equivalent Thorium (eTh) map

The equivalent thorium contour map (Fig. 6) shows that, there are three levels of thorium concentrations. The first low level has eTh values less than 9.05 ppm. This low concentration is coincided with Quaternary wadi sediments and older granites at the eastern parts of the studied area. The second intermediate level (from 9.05 to 12.23 ppm) is recorded over older granites at central to western parts of the studied area. The third high level has value th-concentration reach to 45.84 ppm and encountered over younger granites, Natach volcanic, gneissose granites and pegmatite.

4.4. Equivalent Uranium (eU) map

Uranium map (Fig. 7) shows high presence which is mainly related to younger granites and Natach volcanics. The values of high presence reach to 20.96 ppm. There are three uranium concentration levels that could be distinguished according to their uranium contents. The first level has U-concentration values less than 6.00 ppm and covers northeastern and south to southeastern parts of the studied area covered by Quaternary deposits, metagabbro and older granites. The second level (from 6.00 ppm to 9.48 ppm) is recorded over some parts of older granites and gneissose granites at the central and western parts of the studied area. The third level possesses relatively high concentrations reach to 20 ppm of eU associated with younger granite rocks

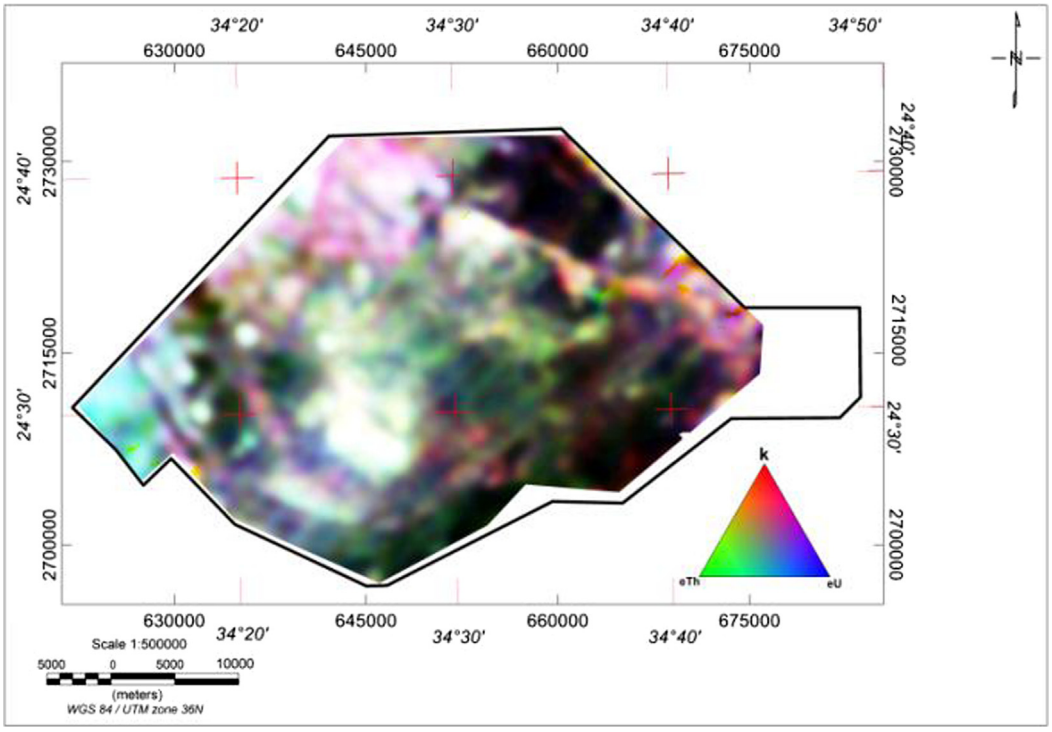

Figure 11 False-color radioelement composite image, G.Abu Had-G.Umm Qaraf area, South Eastern Desert, Egypt.

around G. El Faliq, Natach volcanics at the western parts and pegmatite.

4.5. Equivalent Uranium/equivalent Thorium (eU/eTh) map

The careful examination of equivalent uranium/equivalent thorium (eU/eTh) color map (Fig. 8) shows that, the distribution of the eU/eTh values is variable and spread over most geological units, in the form of dispersed anomalies scattered in intermediate eU/eTh background. The lowest values (less than 0.64) are related to gneissose granite rocks, some localities of older granites and Quaternary deposits at the central parts of the studied area. Meanwhile, the highest values (more than 0.7) are recorded over younger granites, pegmatite and older granites at the eastern parts. The increase of eU/eTh values may be related to the uranium leaching process, since it is mobile and leachable, if it is compared with thorium which is stable.

4.6. Equivalent Uranium/Potassium (eU/K) map

The eU/K map (Fig. 9) shows that, the distribution of the eU/K values is variable and spread over most geological units, reflecting two levels of this ratio. The lowest values (less than 3.9) are recorded in many parts of the studied area. These values are observed over gneissose granites, older granites and wadi deposits. Meanwhile, the highest values (more than 4.7) are recorded in the western part as well as spots in southern and northeastern parts. These are covered Natach volcanic, younger granitic rocks and pegmatites.

4.7. Equivalent Thorium/Potassium ratio (eTh/K) map

In the eTh/K contour map (Fig. 10) the relatively high eTh/K concentration is associated with gneissose granitic rocks, younger granites and Natach volcanics. These high anomalies (more than 6.4) are concentrated in the western part, zones in southern and at central of the studied area. Meanwhile, the lowest values (less than 6.4) are observed generally in the northern and eastern parts. The low value is observed over spots of older granite rocks, serpentinite rocks and Quaternary wadi deposits.

4.8. Radioelement composite image

Different rock types have different characteristic concentrations of radioelements, potassium, uranium and thorium. Therefore, concentrations calculated from gamma ray spectrometric data can be used to identify zones of consistent lithology and contacts between constraining lithologies.

The three radioelements composite image map (Fig. 11) of the study area shows the variations occurring in the three radioelements concentrations, which mainly reflect lithologic variations. This map is composed with display of equivalent uranium (ppm), equivalent thorium (ppm) and potassium (%). The color index at each corner of the triangular legend (K in red, eU in blue and eTh in green) indicates 100% concentration of the indicated radioelements.

The observed radioelement map shows a fairly close spatial correlation with the geological map presented in Fig. 2. The high values directed in bright color are related to younger

Table 1 Rock units statistical values which will be used to apply the statistical tests for TC radiometric distributions.

No.	Units	Number of reading	Minimum μR/h	Maximum μR/h	Mean	Standard deviation
1	QW	23333	5.39	30.40	14.01	3.86
2	T	95	14.98	20.08	16.57	1.04
3	Nv	937	8.56	42.83	18.12	4.53
4	gm	662	11.73	42.85	20.29	7.04
5	P	323	12.76	27.01	19.96	3.48
6	mgb	3350	5.303	34.39	15.91	4.51
7	gd	6346	11.32	41.33	19.67	6.06
8	gdf	19092	5.14	37.29	15.02	4.19
9	mva	446	13.77	22.77	16.51	1.63
10	osp	260	10.34	25.24	16.78	4.32

Table 2 Summary of the results of χ^2-test of the TC measurements collected over the area.

No.	Rock unit	Theoretical chi	Calculated chi	K	Normality
1	QW	24.68	26.48	15	Normal
2	T	13.23	13.06	7	Normal
3	Nv	20.48	18.56	10	Normal
4	gm	20.48	18.38	10	Normal
5	P	16.92	16.39	9	Normal
6	mgb	21.03	20.86	12	Normal
7	gd	22.36	25.51	13	Not Normal
8	gdf	24.68	26.48	15	Normal
9	mva	16.92	15.89	9	Normal
10	osp	16.92	16.31	9	Normal

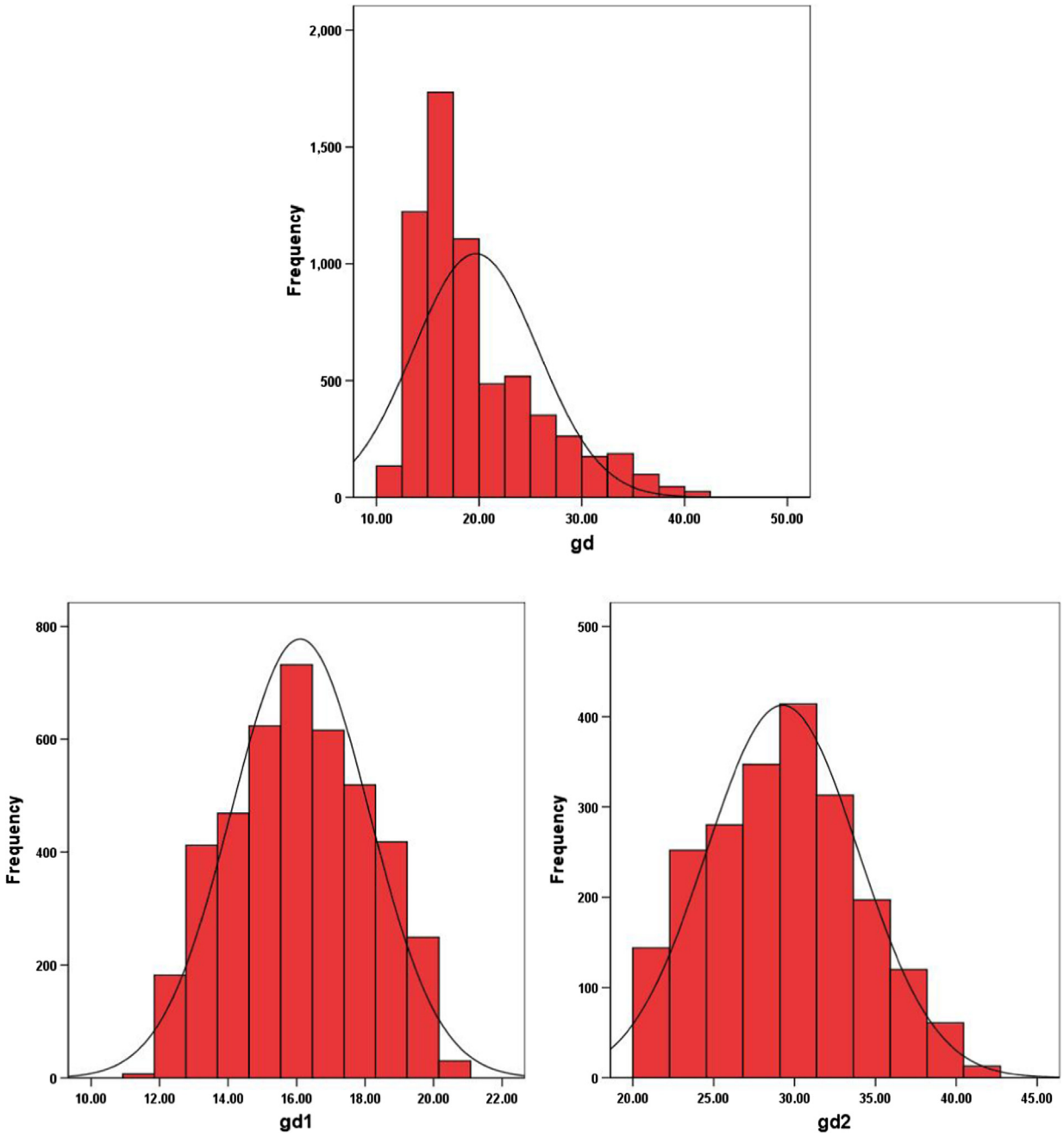

Figure 12 Frequency distribution histograms of the aerial total-count concentrations with their fitted theoretical curves of gneissose granites (gd) and subdivided units of gneissose granites (gd1 and gd2).

Table 3 Summary of the results of χ^2-test of the TC measurements for the two not normal rock units.

Rock unit	Sub-unit	*N*	mini	maxi	*X* mean	ST.D	Theoretical chi	Calculated chi	K	Normality
gd	gd1	4258	11.33	20.28	16.10	2.01	21.46	21.26	12	Normal
	gd2	2141	20.20	41.33	29.25	4.70	19.55	19.38	11	Normal

granite, gneissose granite, pegmatite and Natach volcanic. They are normally characterized by their strong radiometric response, are clearly visible on the composite radioelement image, and can be easily discriminated from the low radioactive rocks. These deposits show a strong spatial correlation with the zones of anomalous high eU, eTh, and K background concentration levels. The high value of eU, eTh and K concentrations is related to basement rock which is presented by

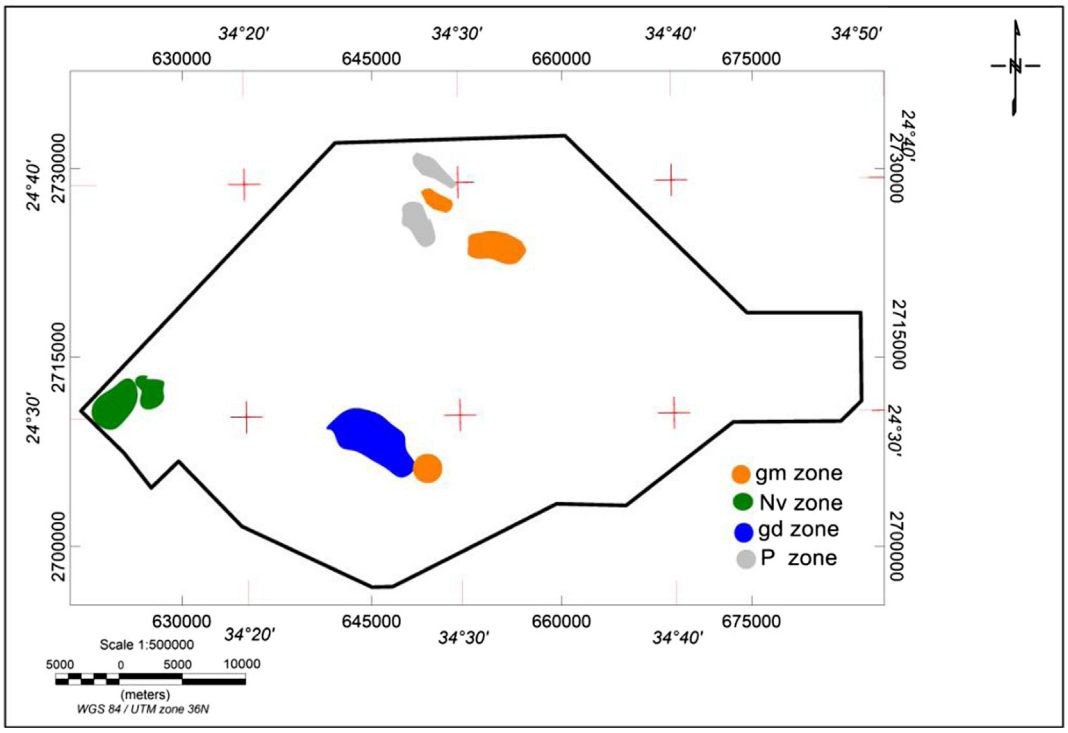

Figure 13 Locations of radioelement anomalies ($X + 3S$), G.Abu Had-G.Umm Qaraf area, South Eastern Desert, Egypt.

white color. The younger granite at Gabal El Faliq, parts of gneissose granites, and Natach volcanics acidic intrusions of pegmatite are clearly distinguishable, in the radioelement composite image (Fig. 11), with white color reflecting relatively high background concentration of the three radioelements.

Low concentrations of eU, eTh and K show dark areas (Fig. 11). This indicates essentially a remarkable spatial correlation with areas covered by Quaternary deposits, exposure older granite, metagabbro and metavolcanics. These zones display a sharp color contrast with the bright colored zones. This reflects the great difference in the radioelement content of the two zones. The radioelement composite image provides on one display an overall pattern of the radioelement distribution. This image offers much in term of lithologic discrimination based on color differences. Also the pale blue color of the west part is indication for uranium enrichment in Natach volcanics.

5. Statistical analysis

5.1. Test of homogeneity (chi-square "χ^2" test)

The radiometric data were statistically analyzed and the results are collected in Table 1. The chi-square (χ^2) test is carried out to test the degree of goodness of fit between the normal (theoretical) curve and the observed one. This test is used to measure the normality of the distribution by applying the following formula (Dixon and Massey, 1957).

$$\chi^2 = \sum_{i=1}^{i=k} (f_i - F_i)^2 / F_i$$

where

χ^2 = chi-square value,

k = total number of class intervals,

f_i = actual number of observations in the ith category, and

F_i = theoretical frequency in the ith category.

The aerial spectral radiometric data were collected and organized over the various exposed rock units in the area under study. The data for each rock unit -after applying the homogeneity χ^2-test-have been analyzed statistically. The data were tabulated in the form of frequency histograms. The arithmetic mean (X) and the standard deviation (S) for each rock unit were computed. The background was designated as all values falling within the limits of three standard deviation from the mean ($X \pm 3S$). This limit was chosen because of the fact that 99.73% of all values in any normal frequency distribution should fall within this range. Any value beyond these limits was considered as anomalous and statistically significant.

5.2. Discussion of the statistical data

By applying of normality test and calculation of chi square test for every rock unit spectrometric data, it is found that there are some units have normal distribution and others have not (Table 2). This is due to the presence of radiometric enrichment in some parts than in the others which may be related to contacts between units and differentiation in mineral distributions. Histogram is a useful method for exploring the shape of distribution of variable values. The rock units and their subunits are represented in Fig. 12. It is found that one unit is divided into two radiometric subunits as the following:

1-Gneissose granite is divided statistically into low total count and high total count values "gd1" and "gd2" respectively. "gd1" has a normal curve at category ($k = 12$) and "gd2" has a normal curve at category value ($k = 11$) (Table 3).

6. Identification and significance of radioelement anomalies

The main target of aerial prospection using gamma ray spectrometric survey data is the delineation of expected boundaries of radioactive concentrations, in which the varying rock units are enriched in eU, eTh and K (Saunders and Potts, 1976). Significant locations of eU, eTh and K anomalies are defined on the basis of calculation of probabilities, where their data differ significantly from the mean background, as defined by the data themselves, and at certain levels of probabilities. The high anomalous values are considered as the values equaling or exceeding at least one standard deviation, two standard deviations and three standard deviations from the calculated arithmetic mean values [$(X + S)$, $(X + 2S)$ and $(X + 3S)$] for eU, eTh and K measurements for each statistically normal rock unit. This could be considered as anomalous values according to Saunders and Potts' (1976) technique for calculating the significant factor of each radiospectrometric variable in each rock unit.

The relatively high anomalies map (Fig. 13) shows locations of statistically high radioelement abundance at four geological rock units. They are associated with relative high eU, eTh and K % elements. These locations are associated with the interpreted composite map. The relatively high values of eU reach 18.95 ppm in younger granites (gm), 19.04 ppm in Natach volcanic (Nv), 18.96 in gneissose granites (gd) and 17.91 ppm in pegmatite. Also the relatively high value eTh reach 45.27 ppm in younger granites (gm), 40.71 in Natach volcanic (Nv), 41.29 in gneissose granites (gd) and 39.73 ppm in pegmatite (P). The relatively high values of K % reach 5.65% at gneissose granites (Table 4).

7. Ground follow-up

The ground follow-up was applied to the relative high radiation at the determined localities younger granites (gm), gneissose granites (gd) and pegmatite (P). This field follow-up can't be applied to Natach volcanics (Nv) because of safety regulations. The field follow-up was done in March 2016.

7.1. Result of measuring field anomaly

The relative high values of eU in ppm, eTh in ppm and K % have been measured and correlated with the airborne gamma-ray survey. The leads of radioelements are correlated with geological rock units (according to the surface geological map). It is found that the radioactive content of the measured rock units is much closed relatively. This will be analyzed at the following discussion:

Table 4 The calculated high radioactive values.

Units	Radioelements	$X + S$	$X + 2S$	$X + 3S$
Younger granites (gm)	eU	18.95	–	–
	eTh	24.72	32.47	40.22
	K	3.42	4.33	5.24
Natach volcanic (Nv)	eU	16.75	19.04	–
	eTh	19.59	23.84	28.09
	K	2.34	2.75	3.16
Gneissose granites (gd)	eU	16.86	18.96	–
	eTh	22.4	28.56	34.72
	K	3.34	4.22	5.1
Pegmatite (P)	eU	15.94	17.91	–
	eTh	16.67	19.07	21.47
	K	3.41	4.12	–

Table 5 Ground spectrometric follow-up for gneissose granite rock of G.Abu Had-G.Umm Qaraf area, South Eastern Desert, Egypt.

R. U.	P	Longitude	Latitude	Airborne data				Field data			
				TC μR/h	K %	eU ppm	eTh ppm	TC μR/h	K %	eU ppm	eTh ppm
gd	1	34°25′43″	24°28′47″	30.44	3.89	16.76	36.32	44.57	5.3	20.3	47.2
	2	34°26′39″	24°27′55″	34.23	4.43	15.61	35.31	44.52	4.6	21.3	43.6
	3	34°25′45″	24°28′49″	31.18	4.26	20.36	30.41	48.8	5.5	22.5	38.3
	4	34°25′40″	24°28′32″	30.53	5.08	17.03	33.24	44.78	5.6	24.9	39.8
	5	34°25′43″	24°29′31″	29.63	5.79	18.52	29.88	47.8	6.2	21.1	34.5
	6	34°25′19″	24°28′48″	34.99	4.71	19.11	37.14	43.8	4.3	23.6	43.9
	7	34°25′59″	24°29′01″	35.81	4.82	15.21	35.05	44.24	5.2	19.9	45.2
	8	34°25′50″	24°28′42″	31.25	5.99	16.97	37.21	40.88	4.8	23.2	41.02
	9	34°26′48″	24°28′48″	29.23	5.91	17.71	34.56	51.3	5.1	21.5	40.21
	10	34°26′46″	24°27′52″	32.06	4.10	18.18	40.21	50.45	4.6	19.2	39.89
	11	34°26′23″	24°29′02″	36.33	4.89	15.51	38.30	42.72	5.3	18.9	42.8
	12	34°26′10″	24°32′03	31.18	4.26	19.36	29.89	48.89	4.7	19.9	33.1

Table 6 Ground spectrometric follow-up for younger granite rock of G.Abu Had-G.Umm Qaraf area, South Eastern Desert, Egypt.

R.U.	P	Longitude	Latitude	Airborne data				Field data			
				TC μR/h	K %	eU ppm	eTh ppm	TC μR/h	K %	eU ppm	eTh ppm
gm	1	34°30′19″	24°37′39″	35.82	4.55	18.24	36.04	48.3	5.6	22.5	38.2
	2	34°31′46″	24°37′25″	38.05	4.56	17.62	36.03	48.32	5.6	23.1	42.5
	3	34°31′44″	24°37′24″	29.15	5.02	20.75	37.5	45.60	5.9	18.5	41.3
	4	34°32′02″	24°37′39″	37.32	5.17	19.17	34.32	46.32	4.8	20.4	45.2
	5	34°32′11″	24°37′31″	34.87	4.51	18.89	35.72	49.16	5.8	23.4	47.5

Table 7 Ground spectrometric follow-up for pegmatite of G.Abu Had-G.Umm Qaraf area, South Eastern Desert, Egypt.

R. U.	P	Longitude	Latitude	Airborne_data				Field data			
				TC μR/h	K %	eU ppm	eTh ppm	TC μR/h	K %	eU ppm	eTh ppm
P	1	34°27′57″	24°39′55″	27.53	4.24	18.84	29.86	39.2	4.9	19.1	37.5
	2	34°30′39″	24°37′34″	26.95	4.23	17.50	28.68	32.14	5.2	19.5	38.3
	3	34°28′30″	24°40′10″	27.36	3.69	15.22	29.21	43.6	3.9	17.2	39.2
	4	34°29′01″	24°39′41″	26.32	3.87	18.06	30.25	47.25	5.5	18.9	37.6

1. Ground follow-up for gneissose granites (gd)

This rock unit has a relative high value of radiometric elements in specific location). These locations have been measured and illustrated at Table 5.

2. Ground follow-up for younger granites (gm)

The younger granite has been checked at many locations, Table 6. These locations are only three site check because of high and mountainous area.

3. Ground follow-up for Pegmatite (P)

The field measurements of pegmatite were applied at these locations (Table 7).

8. Conclusion

Airborne gamma ray spectrometric measurements provide a good method for mapping surface geology of the studied area. In this work the radioelements (K, eTh, and eU), their ratios and total count radiometric maps were interpreted. The radioactive contents of each rock units were statistically analyzed. Also field follow-up was applied to verify the relatively high anomalies of radiometric content which are related to younger granites, Natach volcanic, gneissose granites and pegmatite. The present study recommends a detailed ground study for these rocks which represent the highest content of uranium in the studied area.

Acknowledgments

I wish to express my deep thanks and gratitude to Airborne Geophysics Group (NMA) for their help and encouragement during the course of this work.

References

Dixon, W.J., Massey, F.J., 1957. Introduction to Statistical Analysis. McGraw-Hill Book Company, Inc., New York, Toronto, London, p. 488.
EGSMA, 1997. Geologic Map of G. Hamata, South Eastern Desert, Egypt. Geologic Survey of Egypt, Cairo.
EGSMA, 2001. Geologic Map of W. Shait, South Eastern Desert, Egypt. Geologic Survey of Egypt, Cairo.
Essa, W.H.M.H., 2015. Analysis and Interpretation of Airborne Magnetic and Gamma-Ray Spectrometric Survey Data of Gabel Umm Tineidba Area, South Eastern Desert, Egypt MSc. in Geophysics. Al-Azhar University.
Druker, Eugene, 2016. Processing of Airborne Gamma-Ray Spectra: Extracting Photopeaks. Report Geoconvention, Canada.
Hashad, A.H., Sayyah, T.A., El-Kholy, S.B., Youssef, A., 1982. Geological and petrological study of Wadi Natach Late Cretaceous volcanics. Egypt. J. Geol. 26, 19–37.
Mostafa, D.A., 2013. Mineralogical and Geochemical Studies of Gabal El-Faliq Granites, South Eastern Desert, Egypt Msc in Geology.
Nuclear Materials Authority, 2012. High-resolution Airborne Gamma-Ray Spectrometric and Aeromagnetic Survey Data over Abu Rushed Area, South Eastern Desert, Egypt Technical Report.
Saunders, D.F., Potts, M.J., 1976. Interpretation and application of high sensitivity airborne gamma ray spectrometric data. In: IAEA Symp. Exploration for Uranium Ore Deposits, Vienna, pp. 107–124.